BIOCHEMISTRY
including biophysical chemistry & molecular biology
Article

Biochemistry **2009,** *48,* 7089–7097 7089
DOI: 10.1021/bi900559k

A Sequential Binding Mechanism in a PDZ Domain†

Celestine N. Chi,‡ Anders Bach,§ Åke Engström,‡ Huiqun Wang,‡ Kristian Strømgaard,§ Stefano Gianni,*,∥ and Per Jemth*,‡

‡*Department of Medical Biochemistry and Microbiology, Uppsala University, BMC Box 582, SE-75123 Uppsala, Sweden,* §*Department of Medicinal Chemistry, University of Copenhagen, Universitetsparken 2, DK-2100 Copenhagen, Denmark, and* ∥*Istituto Pasteur-Fondazione Cenci Bolognetti and Istituto di Biologia e Patologia Molecolari del CNR, Dipartimento di Scienze Biochimiche "A. Rossi Fanelli", Sapienza Università di Roma, Piazzale A. Moro 5, 00185 Rome, Italy*

Received April 2, 2009; Revised Manuscript Received May 19, 2009

ABSTRACT: Conformational selection and induced fit are two well-known mechanisms of allosteric protein−ligand interaction. Some proteins, like ubiquitin, have recently been found to exist in multiple conformations at equilibrium, suggesting that the conformational selection may be a general mechanism of interaction, in particular for single-domain proteins. Here, we found that the PDZ2 domain of SAP97 binds its ligand via a sequential (induced fit) mechanism. We performed binding experiments using SAP97 PDZ2 and peptide ligands and observed biphasic kinetics with the stopped-flow technique, indicating that ligand binding involves at least a two-step process. By using an ultrarapid continuous-flow mixer, we then detected a hyperbolic dependence of binding rate constants on peptide concentration, corroborating the two-step binding mechanism. Furthermore, we found a similar dependence of the rate constants on both PDZ and peptide concentration, demonstrating that the PDZ2−peptide interaction involves a precomplex, which then undergoes a conformational change, and thereby follows an induced fit mechanism.

Proteins are dynamic molecules that are constantly in contact with thousands of other protein molecules in the cell in a highly dynamic process. Interactions within and between these proteins are essential for function. Understanding the mechanisms through which proteins interact with their ligands is important given that many of these proteins are targets in drug development. The binding mechanism of some proteins could be described by a simple one-step bimolecular association, whereas others involve conformational changes, which were classically formalized in the Monod−Wyman−Changeaux (MWC) concerted mechanism (*1*) and the Koshland−Nemethy−Filmer (KNF) model (induced fit or sequential mechanism) (*2*). These models were originally applied to multidomain proteins and to equilibrium experiments. Today, it has been recognized that allosteric mechanisms operate in single protein domains as well, for example, through the conformational selection model (also called selected fit, conformational sampling) (*3*), which assumes the existence of a protein molecule in an ensemble of several different conformations, which are in rapid equilibrium. In the presence of a ligand, a high-energy conformation with high affinity binds the ligand and causes the equilibrium to shift toward the favored conformation, i.e., that of the final protein complex (*4*−*6*). This model is consistent with the statistical theory of protein folding in which a protein continuously samples a range of substates whose statistical weights are redistributed upon binding (*7*, *8*). On the other hand, in the induced fit model, interaction between the protein and the ligand leads to a precomplex that undergoes structural rearrangements to form the final complex. In the absence of solution kinetics, both models are plausible (*6*, *9*, *10*), especially when only the bound and unbound forms in the crystal structures are examined.

Recently, using residual dipolar couplings, Lange et al. (*3*) extracted an ensemble of conformations representing 46 known X-ray structures of ubiquitin, suggesting that this protein recognizes its ligands through conformational selection. A similar conclusion was reached by Gsponer et al. (*11*), who used molecular dynamics simulation restrained by experimental NMR data (S^2 order parameters and NOE-derived interproton distances) and found preexisting binding-competent conformations for calmodulin. This notwithstanding, there is a substantial amount of experimental evidence in support of the induced fit mechanism for various proteins (*4*, *12*, *13*), and a protein may

†This work was supported by grants from the Swedish Research Council, Magnus Bergvall's foundation, OE and Edla Johansson's foundation, Carl Trygger's foundation, Jeansson's foundation, Clas Groschinskys minnesfond and the Medical Faculty, Uppsala University (to P.J.), the Lundbeck Foundation (to K.S.), and the Drug Research Academy, Faculty of Pharmaceutical Sciences, University of Copenhagen (Ph.D. scholarship to A.B.)

*To whom correspondence should be addressed. S.G.: Istituto Pasteur-Fondazione Cenci Bolognetti and Istituto di Biologia e Patologia Molecolari del CNR, Dipartimento di Scienze Biochimiche "A. Rossi Fanelli", Sapienza Università di Roma, Piazzale A. Moro 5, 00185 Rome, Italy; e-mail, Stefano.Gianni@uniroma1.it; fax, +39-064440062; phone, +39-0649910548. P.J.: Department of Medical Biochemistry and Microbiology, Uppsala University, BMC Box 582, SE-75123 Uppsala, Sweden; e-mail, Per.Jemth@imbim.uu.se; fax, +46-18-471 4209; phone, +46-18-471 4557.

Published on Web 06/04/2009

both sample different conformations and undergo an induced fit (*5*, *6*, *14*). It has thus been established that allostery is important for the function of single protein domains. Such allostery may involve the redistribution of states (substates) that are in equilibrium, or even side chain and backbone dynamics without a conformational change (dynamic allostery) (*11*, *15*−*19*). To determine which allosteric mechanism that is being used by a protein is not only of academic interest. For example, when the rational design of drugs is being conducted, it is important to know whether the averaged NMR structure or crystal structure is the drug target or if there is another high-affinity conformer, which should be considered.

In this study, we experimentally address the question of conformational selection and/or induced fit in the binding event between a peptide ligand and a PDZ domain. PDZ domains are protein modules of 80−100 amino acids involved in protein−protein interactions (*20*). They have been shown to mediate binding to the C-terminus of other proteins, where conserved interactions with the C-terminal carboxylate of the ligand are important. PDZ domains are considered to be relatively promiscuous because of their broad range of specificities (*21*, *22*). A priori, a protein such as the PDZ domain, which binds several different ligands, would appear likely to bind ligands through conformational selection. Indeed, previous work on PDZ domains using NMR demonstrated long-range effects on the side chain dynamics consistent with this idea (*23*).

Here, we combined site-specific mutagenesis in SAP97 PDZ2 with kinetic ligand binding experiments (stopped-flow and continuous-flow fluorimetry) to show that the minimal scheme describing the SAP97 PDZ2−peptide interaction is a two-step mechanism, where there is an initial complex, which then undergoes a conformational change via the induced fit mechanism.

MATERIALS AND METHODS

cDNA Constructs. The cDNA encoding PDZ2 of SAP97 (residues 311−407) was amplified by polymerase chain reaction (PCR) and cloned into EcoRI and BamHI sites of a modified His-tagged pRSET vector (Invitrogen). Mutants were generated by inverted PCR. The expressed PDZ domain contained a His tag (MHHHHHLVPRGS) in the N-terminus and a C378A mutation to prevent disulfide bridges. We have previously shown for other PDZ domains that this His tag does not influence PDZ binding or stability (*24*, *25*). The C378A mutation also did not influence the stability of the protein (not shown).

Peptide Synthesis. Peptides were either bought from JPT (Dansyl-RRETQV) or manually synthesized [18E6C$_{WT}$ (LQRRRETQV), 18E6C$_{Leu}$ (LQRRRETQL), and 18E6C$_{Abu}$ (LQRRRETQAbu, where Abu is aminobutyric acid)] by Fmoc-based solid-phase peptide synthesis (SPPS) using a Mini-Block (Mettler, Toledo, OH) as described previously (*25*). Briefly, after crude peptides were synthesized, Fmoc deprotection was performed with 20% piperidine in DMF (2 × 10 min), and coupling of the consecutive amino acid was carried out with 2-(1*H*-benzotriazol-1-yl)-1,1,3,3-tetramethyluronium hexafluorophosphate (HBTU) and DIPEA (1:4:4:4 resin/amino acid/HBTU/DIPEA mixture) and monitored by the ninhydrin test. The final peptide was cleaved off the resin by treatment with 5% water and 5% triisopropylsilane in trifluoroacetic acid (TFA) for 2 h. The crude peptide was analyzed by liquid chromatography−electrospray ionization mass spectroscopy (LC−ESI-MS) and purified by preparative HPLC to >98% purity. The final peptide solution was analyzed by LC−ESI-MS and lyophilized. The concentration of the peptide in solution was determined by amino acid analysis.

Expression and Purification. Protein expression was as previously described (*26*). Briefly, competent *Escherichia coli* bacteria [BL21(DE3)pLysS] were transformed with PDZ-expressing constructs and grown at 37 °C to an OD_{600} of 0.6. Protein expression was then induced with 1 mM IPTG, and the protein was expressed overnight at 30 °C. Purification of PDZ was conducted as described previously (*26*); however, after elution from the nickel column, PDZ-containing fractions were pooled, concentrated, and further purified on a G-50 Sephadex (GE Healthcare) gel filtration chromatography column equilibrated with 100 mM sodium phosphate (pH 7.0). The purity of the PDZ was checked via sodium dodecyl sulfate−polyacrylamide gel electrophoresis (SDS−PAGE) stained with Coomassie brilliant blue and their identity confirmed by matrix-assisted - laser desorption ionization time-of-flight mass spectrometry (Maldi-Tof).

Stability Measurements. Stability estimates were conducted by urea-induced equilibrium denaturation experiments. We performed measurements at 25 °C in 50 mM potassium phosphate (pH 7.45) by increasing the urea concentration at a constant PDZ concentration (5 μM) and recording the fluorescence at different emission wavelengths upon excitation at 280 nm. The data were fitted to the general equation for solvent denaturation of a two-state protein (*27*) to generate equilibrium constants for the PDZ domains. Far-UV circular dichroism experiments were performed in a Jasco J-810 spectropolarimeter. Spectra were recorded between 200 and 260 nm at 25 °C in 50 mM potassium phosphate (pH 7.45) at protein concentrations of 20−45 μM.

Binding Experiments. All binding experiments were conducted in 50 mM potassium phosphate (pH 7.5). Equilibrium measurements were performed by measuring the increase in tryptophan fluorescence upon binding at 25 °C, in an SLM 4800 spectrofluorimeter (SLM instruments). Excitation was at 280 nm and emission at 340 nm. In a typical equilibrium binding experiment, different concentrations of peptide or PDZ in buffer were added to a constant concentration of PDZ or peptide (5 or 10 μM respectively), and the change in fluorescence was measured. The data were then fit to the standard quadratic equation (*28*) to determine the K_D value. Stopped-flow measurements were taken at 10 or 25 °C on an SX-20MV stopped-flow spectrometer (Applied Photophysics, Leatherhead, U.K.). Fluorescence was monitored using (i) the increase in tryptophan fluorescence upon binding of the unlabeled peptide (excitation at 280 nm, emission at >320 nm), (ii) the decrease in tryptophan emission upon binding of dansylated peptide (excitation at 280 nm, emission between 320 and 465 nm), and (iii) the increase in dansyl fluorescence due to FRET around 550 nm (excitation at either 280 or 345 nm, emission at >475 nm). Slit widths were 4 nm for both the entrance and the exit of the monochromator. Varied amounts of peptide or PDZ were rapidly mixed with a constant amount of PDZ (5 μM, when using unlabeled peptide and monitoring the tryptophan in the PDZ) or dansylated peptide (5 μM), respectively, and the change in fluorescence was measured over time. Traces of fluorescence versus time were fitted to a single- or double-exponential equation, and one or two observed rate constants were thus obtained. Observed rate

constants were then plotted against the concentration of the varied species and microscopic rate constants for the slow phase λ_2 at 10 °C determined by fitting the data to the equation for a bimolecular association (eq 1) (*24*, *29*).

$$k_{obs} = [k_{on}^2(n - [A]_0)^2 + k_{off}^2 + 2k_{on}k_{off}(n + [A]_0)]^{0.5} \quad (1)$$

where k_{on} is the observed association rate constant, k_{off} is the observed dissociation rate constant, and $[A]_0$ and n are the initial concentrations of the varied and constant species, respectively. In the chase experiment described in Results, observed rate constants were fitted to eq 2 to estimate the apparent, or net, off rate constant for the dansylated peptide, k_{off}^{app}.

$$k_{obs} = k_{off}^{app} + k_{on}' \times K_D/(K_D + [\text{unlabeled peptide}]) \quad (2)$$

where K_D is the dissociation constant for the PDZ and the unlabeled peptide and k_{on}' the apparent (first-order) on rate constant for the labeled peptide and the PDZ domain at the chosen concentration of labeled peptide. (Only k_{off}^{app} can normally be accurately estimated from this experiment.)

Continuous-flow measurements were performed at 25 °C as previously described (*13*). Briefly, PDZ (5 μM when the peptide concentration was varied) and peptide (5 μM when the PDZ concentration was varied) were rapidly driven into the flow cell, which was illuminated with an A1010B mercury−xenon lamp at 280 nm. Fluorescence was monitored with a Micromax CCD camera (Princeton Instrument), at >475 nm with an exposure time of 2−3 s. A typical binding trace was plotted after taking into account the background fluorescence and fitted to a single-exponential time course. Observed rate constants were plotted against both peptide and PDZ concentration, and fitted together to eq 3.

$$k_{obs} = k_{off}^{app} + k_2 \times [\text{ligand}]/(K_{0.5} + [\text{ligand}]) \quad (3)$$

where k_2 is the rate constant for the conformational change (see Figures 5 and 6) and $K_{0.5}$ an apparent dissociation constant composed of several microscopic rate constants. In the curve fitting, the k_{off}^{app} was constrained to 35 s^{-1} as determined separately in the experiment in which the dansylated peptide was chased out by an excess of unlabeled peptide ligand. Experimental data were analyzed with Kaleidagraph version 4.0 (Synergy software) or Prism version 4.0 (GraphPad).

RESULTS

We are interested in whether induced fit and/or conformational selection is present in binding events of protein domains. Here, we have used PDZ2 from SAP97 because four determined and slightly different structures are available for this protein domain (*30*−*32*) (Figure 1). Ligand-bound and ligand-free crystal structures also differ, most notably in the βA−βB loop, and this result has been interpreted in terms of the sequential model (*32*). In general, PDZ domains are promiscuous, and one can assume that there are different substates with different affinities for different ligands (*33*, *34*). We therefore investigated the putative two-step binding mechanism of the SAP97 PDZ2−ligand interaction to address the question of conformational selection versus induced fit. As a ligand for the PDZ domain, we used a peptide derived from the C-terminus of the human papillomavirus 18 (HPV-18) E6 protein. The E6 protein of oncogenic HPV strains contains a conserved C-terminal sequence that binds to PDZ domains

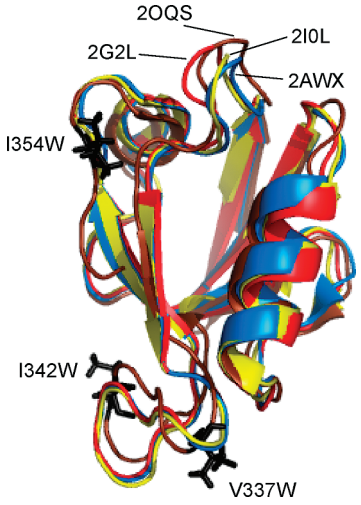

FIGURE 1: To show the tentative diversity of conformations of SAP97 PDZ2, with and without ligand, we superimposed backbone atoms from PDZ in complex with peptide [Protein Data Bank (PDB) entries 2G2L (red), 2I0L (yellow), and 2OQS (chocolate)] and unliganded PDZ [AWX (marine blue)]. Also shown in black are the side chains of I354, I342, and V337, which were mutated to tryptophans in this study. This picture was drawn with PyMol (*46*).

and targets PDZ-containing proteins for proteosomal degradation (*35*).

All PDZ variants used in this study were stable and folded as judged by fluorescence-monitored urea denaturation and circular dichroism experiments (Figure 2 and Table 1). To monitor binding events between the peptide ligand and the PDZ domain by tryptophan flourescence as well as Förster resonance energy transfer (FRET), we engineered three mutants of SAP97 PDZ2: V337W, I342W, and I354W (Figure 1). These tryptophan probes served two purposes. First, binding between PDZ and peptide could be measured with Trp fluorescence giving a very high signal-to-noise ratio in the stopped-flow spectrofluorimeter. Second, we could monitor the binding using FRET in a continuous-flow spectrometer.

Initially, we measured the binding kinetics of the SAP97 PDZ2 mutants (V337W, I342W, and I354W) by FRET in the stopped-flow fluorimeter at 10 °C. For this experiment, we first used a dansylated version of the HPV18 E6 peptide (Dansyl-RRETQV) with the minimal sequence known to be required for binding to SAP97 PDZ2 (*31*). Single-exponential fits gave rather poor residuals for all three mutants, and data were thus fitted to a double-exponential equation (Figure 3A). Importantly, observed rate constants were similar for all three mutants, demonstrating that the tryptophans did not affect binding kinetics (Figure 3B). The fast phase λ_1 appeared to be just on the limit of what can be accurately measured with a stopped-flow apparatus (dead time of 1.5 ms) and is therefore not reported in the figure. We then investigated the binding kinetics of I354W with the unlabeled peptide $18E6C_{WT}$ (LQRRRETQV; corresponding to the last nine amino acids of the C-terminus of HPV-18 E6), which was also found to exhibit biphasic binding kinetics, but with a much improved signal-to-noise ratio as compared to that from the FRET experiment (Figure 4A). The contribution from Tyr fluorescence to the observed fluorescence change was negligible (Figure 4D). Consistent with the experiment with dansylated peptide, the fast phase λ_1 obtained with unlabeled peptide was on the limit for

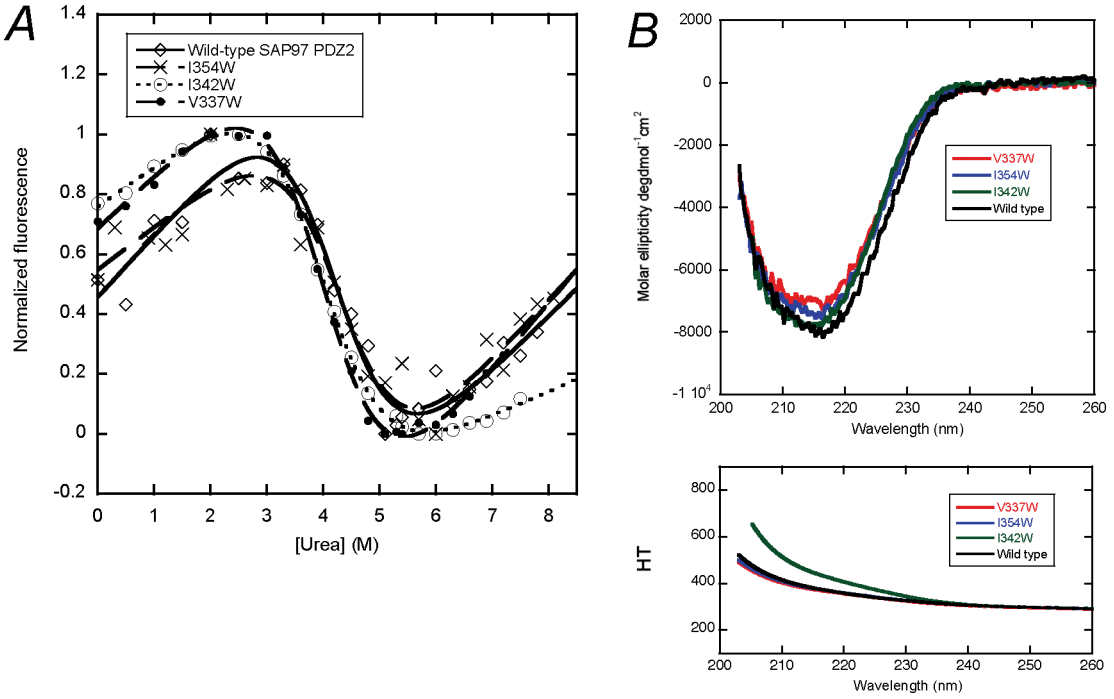

FIGURE 2: Equilibrium data for wild-type and Trp mutants of SAP97 PDZ2. (A) Fluorescence-monitored urea denaturations. In the curve fitting, the m_{D-N} value was shared, demonstrating that all mutants could be fit well to a common value (1.07 ± 0.09 kcal mol^{-1} M^{-1}, fitting error). Free fitting gives m_{D-N} values between 0.95 and 1.15 kcal mol^{-1} M^{-1}, which is within error of this experiment. See Table 1 for parameters from free fitting as well as fitting with the shared m_{D-N} value. (B) Far-UV circular dichroism spectra of PDZ variants. HT is the high-tension voltage that roughly reflects the absorbance of the sample and should not reach saturation.

Table 1: Parameters from Urea Denaturation of Wild-Type and Trp Mutants of SAP97 PDZ2[a]

	m_{D-N} value (shared in fitting) (kcal mol^{-1} M^{-1})	$[\text{urea}]_{50\%}$ (M)	ΔG_{D-N} (kcal/mol)	m_{D-N} value (free fitting) (kcal mol^{-1} M^{-1})	$[\text{urea}]_{50\%}$ (M)	ΔG_{D-N} (kcal/mol)
wild type	1.07 ± 0.09	4.2 ± 0.1	4.5 ± 0.4	1.14 ± 0.24	4.21 ± 0.14	4.8 ± 1.0
V337W	1.07 ± 0.09	4.0 ± 0.1	4.3 ± 0.4	1.15 ± 0.06	4.02 ± 0.03	4.6 ± 0.2
I342W	1.07 ± 0.09	3.9 ± 0.1	4.2 ± 0.4	1.04 ± 0.04	3.94 ± 0.03	4.1 ± 0.2
I354W	1.07 ± 0.09	4.3 ± 0.1	4.6 ± 0.4	0.95 ± 0.21	4.35 ± 0.18	4.1 ± 0.9

[a] The errors for m_{D-N} and $[\text{urea}]_{50\%}$ are from the curve fitting, and the errors for ΔG_{D-N} values are propagated curve fitting errors.

the stopped-flow technique. Therefore, only the rate constants of the slow phase λ_2 were plotted versus increasing peptide concentration (Figure 4E). Similar kinetics were obtained for the V337W and I342W mutants (not shown), again suggesting that the Trp mutations did not influence binding kinetics. Hence, these biphasic kinetics of the interaction of SAP97 PDZ2 with HPV18 E6-derived peptides suggested a binding mechanism different from a simple one-step association.

We then compared the binding kinetics of the I354W mutant and the 18E6C$_{WT}$ peptide with those of peptides in which the C-terminal Val was replaced with either Leu (18E6C$_{Leu}$) or 2-aminobutyric acid (18E6C$_{Abu}$). Binding traces for the modified peptides were described well by single exponentials (Figure 4B, C), which could reflect a decreased energetic barrier for an intramolecular step and a resulting higher λ_1, which could not be detected in the stopped-flow spectrometer. The observed rate constants were plotted versus increasing peptide concentrations together with data for 18E6C$_{WT}$ (Figure 4E and Table 2). The dissociation rate constants increased for both substituted peptides (Table 2), which is expected if the wild-type Val is evolutionarily optimized for fitting into the hydrophobic pocket. Deleting a methyl group (Val to Abu) results in a loss of hydrophobic contacts and lower affinity. The association rate constant for 18E6$_{Leu}$ also seemed to be affected by the peptide mutation, which is less obvious, but consistent with a two-step mechanism involving a conformational change, where the barrier for the intramolecular step is modulated by the mutation (*13*, *20*). However, the k_{on} obtained for the 18E6C$_{Leu}$ peptide should not be overinterpreted because of the large k_{obs} values at high peptide concentrations.

Importantly, the data presented so far could not unequivocally distinguish between conformational selection and induced fit since both models were consistent with the experimental data for λ_1 and λ_2. Therefore, to investigate the mechanism further, we employed an ultrarapid continuous-flow mixer and assessed peptide−PDZ binding using FRET at 25 °C. All binding traces for the PDZ−peptide ligand interaction at different concentrations of the PDZ domain and peptide fitted well to a single-exponential equation [i.e., only the slow phase λ_2 could be monitored (Figure 5A)]. A hyperbolic dependence of the observed rate constants was seen with a rate-limiting value of ~5500 s^{-1} (Figure 5B, eq 3), which is a clear indication of a conformational change. Importantly, we varied the

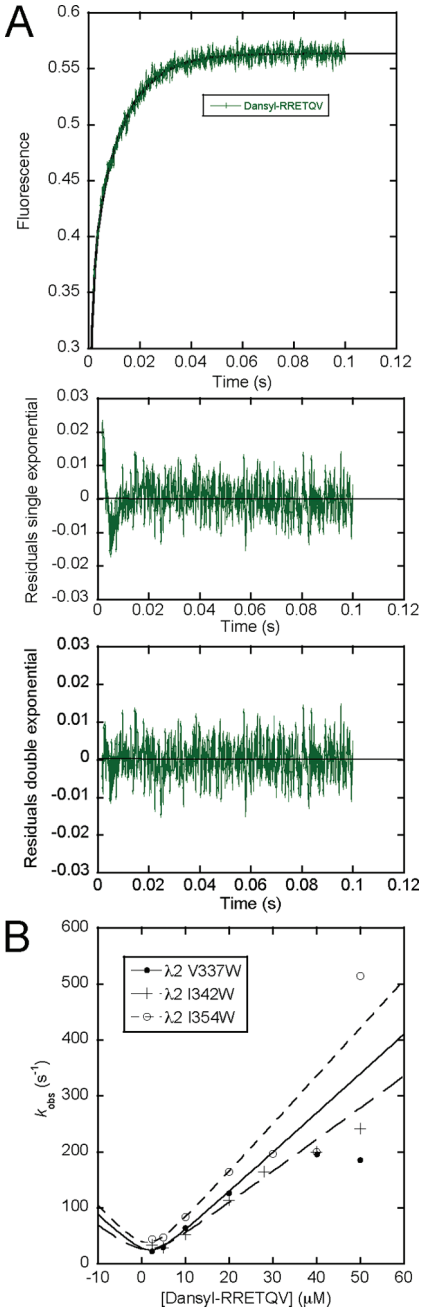

FIGURE 3: Stopped-flow binding traces for PDZ I354W and the peptide Dansyl-RRETQV. The change in fluorescence upon peptide binding was monitored by FRET at >475 nm; excitation was at 280 nm. (A) Data were fitted to a single-exponential (top residuals) or double-exponential (fitted curve and bottom residuals) equation. Traces for V337W and I342W were similar to those of I354W, and observed rate constants for the slow phase λ_2 for all three Trp mutants are plotted vs peptide concentration in panel B. The observed rate constants were fitted to the equation for bimolecular association under second-order conditions (*29*), and parameters are reported in Table 2.

concentrations of both SAP97 PDZ2 I354W and Dansyl-RRETQV, and in both cases, the observed rate constants displayed a similar hyperbolic dependence on peptide or PDZ concentration (Figure 5B). This similarity in concentration dependence implies that the binding mechanism of the SAP97 PDZ2−ligand interaction could be described by a two-step process in which there is an initial encounter complex followed by a conformational change, i.e., induced fit (Figure 6, Scheme I). In the alternative scenario (Figure 6, Scheme II), the PDZ exists in multiple conformations (for the sake of simplicity two), which are in a fast equilibrium and where only one can bind the peptide. If such conformational sampling is considered, we would expect an almost linear increase in the apparent rate constant λ_2 when the concentration of PDZ is increased (while the peptide concentration is kept constant) (*36*), and such behavior was not observed.

From the obtained data, we could estimate microscopic rate constants for this PDZ−peptide interaction at 25 °C. An apparent on rate constant of 2.7×10^7 M^{-1} s^{-1} was calculated from the initial slope of the hyperbolic curve in Figure 5B. We then measured an off rate constant of 35 s^{-1} independently by a "chase experiment" in the stopped-flow. In this experiment, PDZ in complex with Dansyl-RRETQV was mixed with unlabeled peptide, resulting in a single-exponential trace as the dansylated peptide was competed out. At high concentrations of unlabeled peptide, the observed rate constant approached the net off rate constant for the binding reaction (k_{off}^{app}) between Dansyl-RRETQV and SAP97 PDZ2. Furthermore, the equilibrium dissociation constant K_D of the PDZ−peptide complex was calculated from both fluorescence end points of stopped-flow binding experiments and equilibrium binding data at 25 °C to be 1.7 μM. The kinetics of a two-step reaction should be fitted to the two roots of a quadratic equation governed by the four microscopic rate constants, k_1, k_{-1}, k_2, and k_{-2} (cf. Schemes I and II in Figure 6) (*27*). Since we could not measure the fast phase in the continuous flow, we can only speculate about the microscopic rate constants in the induced fit scheme (Scheme I, Figure 6), except the one for the intramolecular step, k_2, which was ~5500 s^{-1}. Given the experimentally determined parameters ($k_{on}^{app} = 2.7 \times 10^7$ M^{-1} s^{-1}, $k_{off}^{app} = 35$ s^{-1}, $k_2 = 5500$ s^{-1}, and $K_D = 1.7$ μM), it can be shown by manual fitting of the observed rate constants in Figure 5B to one of the two roots of the quadratic equation (corresponding to the slow phase) that several scenarios are consistent with the data. For example, transition state 2 could be the main barrier of the binding reaction and free PDZ could be in a rapid pre-equilibrium with the PDZ−peptide intermediate (Figure 6, top diagram). In this scenario, the equilibrium constant for the initial PDZ−peptide interaction would be roughly 0.2 mM and both k_{-1} and k_1 would be large. The heights of TS1 and TS2 might also be similar relative to that of the PDZ−peptide intermediate, and the K_D for the initial encounter would then approach 0.1 mM, as depicted in the middle disgram of Figure 6. This scenario is the most likely as it is consistent with the observation of double-exponential kinetics in the stopped flow at 10 °C. (In the first scenario, λ_1 would be too large to detect in the stopped flow). Finally, TS1 might be higher than TS2 (i.e., $k_{-1} < k_2$), with the apparent association rate constant approaching the true one and the K_D for the initial encounter approaching the overall K_D (Figure 6, bottom diagram). This third scenario is less likely as we then would expect to see clear biphasic kinetics in both the stopped-flow and continuous-flow spectrometer.

DISCUSSION

Since the pioneering work of the early 1960s (*1*, *2*), it has become clear that allostery plays an important role in protein−protein interactions (*37*). With new NMR methodologies for

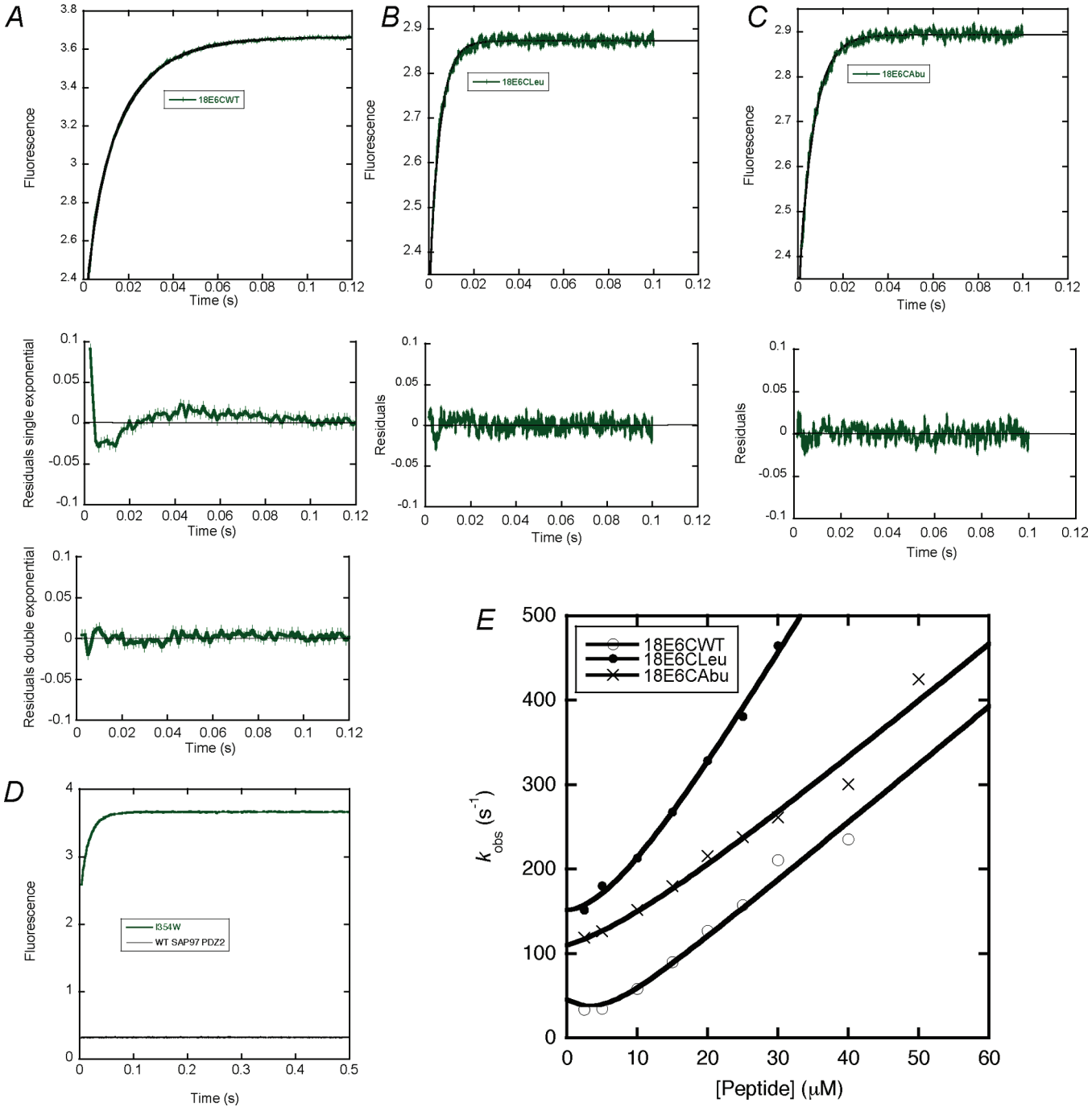

FIGURE 4: Stopped-flow binding traces for PDZ I354W and substituted peptides: (A) 18E6C$_{WT}$ (LQRRRETQV), (B) 18E6C$_{Leu}$ (LQRRRETQL), and (C) 18E6C$_{Abu}$ (LQRRRETQAbu). The change in fluorescence upon peptide binding was monitored at >320 nm, and excitation was at 280 nm. Binding traces for 18E6C$_{Leu}$ and 18E6C$_{Abu}$ fitted well to a single-exponential equation, but kinetics for the 18E6C$_{WT}$ peptide displayed clear biphasic behavior. The residuals are shown below each binding trace. (D) Stopped-flow binding traces for the I354W mutant and wild-type SAP97 PDZ2 demonstrating that the observed change in fluorescence comes from the engineered tryptophan. (E) Observed rate constants for the slower phase λ_2 plotted vs peptide concentration. Data were fitted to eq 1, and parameters are reported in Table 2.

probing dynamics of proteins emerging (*17*, *38*−*42*), the conformational selection mechanism (conformational sampling, selected fit, population shift, etc.) has been put forward as a general mechanism for allostery (*3*, *11*, *15*, *18*). It is clear from structural and dynamic data from NMR experiments that multiple conformers exist for many if not all proteins, especially if the concept of dynamic equilibrium is included (*3*, *17*, *18*, *23*, *38*, *41*, *43*, *44*). Such data obviously suggest that conformational selection is a likely mechanism of binding (*3*). However, we present here direct experimental evidence of an induced fit binding mechanism in a PDZ domain, showing that an intramolecular step subsequent to ligand binding contributes significantly to the binding energy of the complex. Structures can tell whether a conformational change has occurred, and for PDZ domains, it appears that some undergo a structural transition (e.g., ref (*34*)); on the other hand, structural transitions are less obvious in others (e.g., ref (*45*)). To determine the order of events in a two-step binding mechanism, it is necessary to acquire time-resolved data. The kinetic data presented here together with previous work on PTP-BL PDZ2 (*13*, *20*) suggest that the observed allostery in

PDZ domains operates via the induced fit mechanism (Figures 5 and 6). It should be noted that a minor fraction of the molecules might follow a parallel route without being kinetically detectable. The major observable route for SAP97 PDZ2 is, however, via the induced fit mechanism, and it is experimentally very difficult to rule out minor pathways. In addition, very fast sampling of conformations before binding ($\gg$10000 s^{-1}) may be present, but if so, the high apparent association rate constant (2.7×10^7 M^{-1} s^{-1}, which is the lower limit for the true k_{on} at 25 °C) suggests that the peptide binds to a lower-energy conformation. Similarly, there might well be multiple complex conformations (after binding) exchanging at rates that are too fast to detect with our instruments. Such situation will affect neither the analysis nor our main conclusion that the major route for peptide binding is via an induced fit mechanism. In our analysis, we assume the simplest mechanism that is consistent with experimental data, and here this is a single complex conformation.

We propose that all peptides bind SAP97 PDZ2 via the induced fit mechanism. The reason we observe biphasic kinetics only for 18E6C_{WT} but not for 18E6C_{Leu} and 18E6C_{Abu} might be a faster conformational change and a lower second energetic barrier for the two latter peptides (Figure 6), which results in a kinetic phase that is too fast to detect. What is the function of a conformational change in a protein domain such as SAP97 PDZ2? Evolution might have favored a mechanism in which initially there is a fast but unspecific association between the PDZ domain and the ligand resulting in a high-energy complex. The specificity is then provided in the second unimolecular step where the complex is rearranged and specific short-range interactions are formed. This mechanism might allow the PDZ domain to

Table 2: Binding Constants for the SAP97 PDZ2−Peptide Interaction[a]

SAP97 PDZ2 variant/peptide	k_{on} (μM^{-1} s^{-1})	k_{off} (s^{-1})	K_D[b] (μM)
I354W/Dansyl-RRETQV[c]	27 ± 2.0	35 ± 3.0[d]	1.7 ± 0.2
I354W/18E6C_{WT}	6.9 ± 0.4	11 ± 4	1.1 ± 0.3
I354W/18E6C_{Leu}	14 ± 0.4	81 ± 4.5	9.3 ± 0 0.6
I354W/18E6C_{Abu}	6.9 ± 0.4	75 ± 8.4	15 ± 0.5
I354W/Dansyl-RRETQV	8.6 ± 0.2	14 ± 1	1.6 ± 0.12[e]
I342W/ Dansyl-RRETQV	5.7 ± 0.1	9.7 ± 0.5	1.7 ± 0.09[e]
V337W/ Dansyl-RRETQV	7.1 ± 0.2	7.0 ± 0.5	1.0 ± 0.08[e]

[a] All binding experiments were performed at 10 °C except where otherwise indicated. Errors are from the curve fitting. [b] The K_D was determined by fitting kinetic end points to the quadratic binding equation (*24*). [c] Experiment conducted at 25 °C. [d] The off rate constant was determined independently by a chase or displacement experiment. [e] Calculated as the ratio of k_{off} to k_{on}. The true error of k_{off} is normally larger than the fitting error in this type of binding experiment.

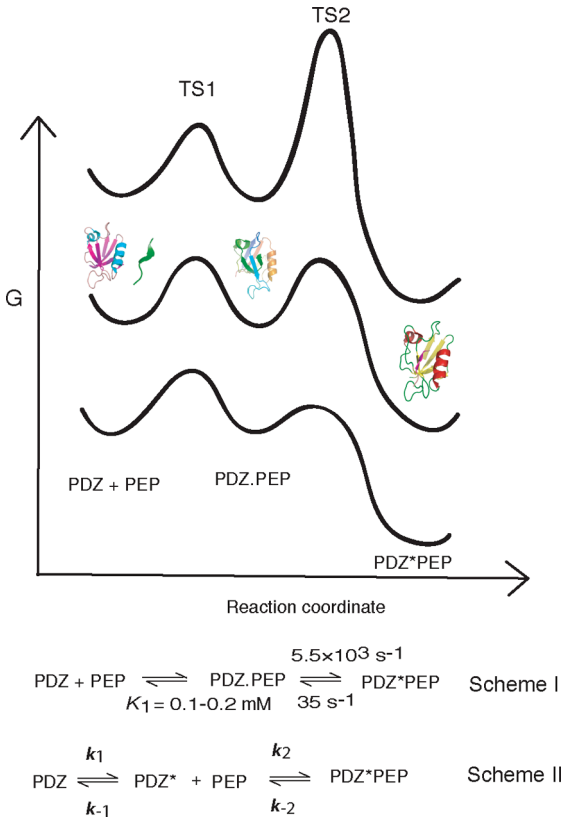

FIGURE 6: Free energy diagram and reaction schemes. A schematic representation of the change in free energy vs reaction coordinate for the SAP97 PDZ2−peptide interaction for the situations in which $k_{-1} \gg k_2$ (top diagram), $k_{-1} = k_2$ (middle diagram), and $k_{-1} < k_2$ (bottom diagram). The relative energy of free PDZ and peptide at a high concentration of peptide (or PDZ) is depicted. Scheme I shows the induced fit mechanism, which is consistent with all our data, whereas Scheme II depicts the conformational selection mechanism. See Results for further discussion of TS1 and TS2, and the estimation of K_D for the initial complex.

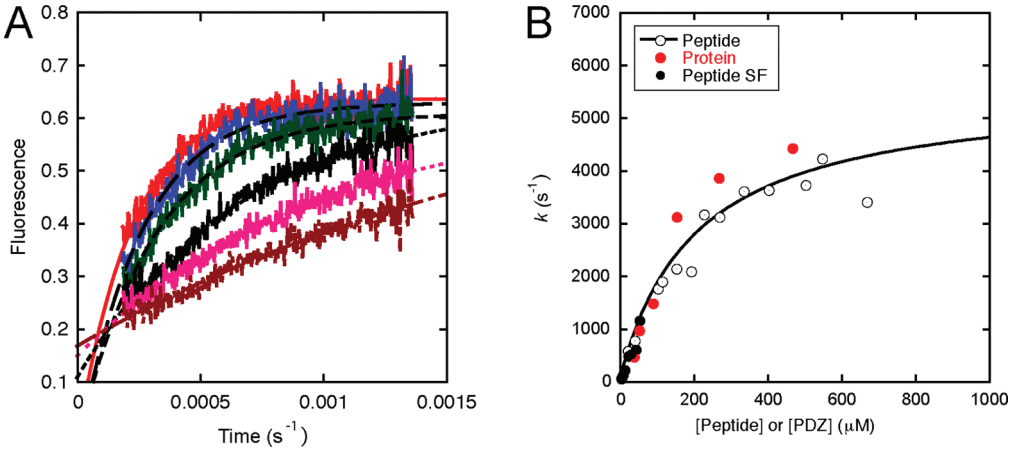

FIGURE 5: (A) Continuous-flow binding traces for the PDZ−peptide (Dansyl-RRETQV) interaction. Binding was assessed with increasing concentrations of the peptide to a constant amount of PDZ (5 μM). The change in fluorescence upon peptide binding was measured by FRET and fitted to a single-exponential equation. (B) Dependence of the observed rate constants on PDZ and peptide concentration. The solid line is a hyperbolic fit of all data points to eq 3: (red circles) PDZ varied, (○) peptide varied, and (●) peptide varied in the stopped-flow spectrometer.

screen a large number of C-termini in the cell (high k_1 and k_{-1}; see Figure 6) and only "lock" those with highest affinity (high k_2 and low k_{-2}).

CONCLUSIONS

We have investigated the kinetic binding mechanism of SAP97 PDZ2 with peptides derived from the C-terminus of the HPV-18 E6 protein. On the basis of kinetic data, SAP97 PDZ2 binds the peptide ligand through an induced fit mechanism. Our results have general implications for the role of allostery in single-domain protein−protein and protein−ligand interactions, where conformational selection often is considered the most plausible mechanism based on multiple conformations detected by NMR methods. While our work does not rule out earlier, fast events, it shows that for SAP97 PDZ2 the major pathway for ligand binding is via a PDZ−peptide precomplex, which undergoes a conformational change to optimize the binding interactions.

REFERENCES

(1) Monod, J., Wyman, J., and Changeux, J. P. (1965) On the Nature of Allosteric Transitions: A Plausible Model. *J. Mol. Biol. 12*, 88–118.

(2) Koshland, D. E.Jr., Nemethy, G., and Filmer, D. (1966) Comparison of experimental binding data and theoretical models in proteins containing subunits. *Biochemistry 5*, 365–385.

(3) Lange, O. F., Lakomek, N.-A., Fares, C., Schroder, G. F., Walter, K. F. A., Becker, S., Meiler, J., Grubmuller, H., Griesinger, C., and de Groot, B. L. (2008) Recognition Dynamics Up to Microseconds Revealed from an RDC-Derived Ubiquitin Ensemble in Solution. *Science 320*, 1471–1475.

(4) Lancet, D., and Pecht, I. (1976) Kinetic evidence for hapten-induced conformational transition in immunoglobin MOPC 460. *Proc. Natl. Acad. Sci. U.S.A. 73*, 3549–3553.

(5) Berger, C., Weber-Bornhauser, S., Eggenberger, J., Hanes, J., Pluckthun, A., and Bosshard, H. R. (1999) Antigen recognition by conformational selection. *FEBS Lett. 450*, 149–153.

(6) Foote, J., and Milstein, C. (1994) Conformational isomerism and the diversity of antibodies. *Proc. Natl. Acad. Sci. U.S.A. 91*, 10370–10374.

(7) Leopold, P. E., Montal, M., and Onuchic, J. N. (1992) Protein folding funnels: A kinetic approach to the sequence-structure relationship. *Proc. Natl. Acad. Sci. U.S.A. 89*, 8721–8725.

(8) Boehr, D. D., and Wright, P. E. (2008) How do proteins interact?. *Science 320*, 1429–1430.

(9) Stevens, F. J., Chang, C. H., and Schiffer, M. (1988) Dual conformations of an immunoglobulin light-chain dimer: Heterogeneity of antigen specificity and idiotope profile may result from multiple variable-domain interaction mechanisms. *Proc. Natl. Acad. Sci. U.S.A. 85*, 6895–6899.

(10) Wilson, I. A., and Stanfield, R. L. (1994) Antibody-antigen interactions: New structures and new conformational changes. *Curr. Opin. Struct. Biol. 4*, 857–867.

(11) Gsponer, J., Christodoulou, J., Cavalli, A., Bui, J. M., Richter, B., Dobson, C. M., and Vendruscolo, M. (2008) A Coupled Equilibrium Shift Mechanism in Calmodulin-Mediated Signal Transduction. *Structure 16*, 736–746.

(12) Bennett, W. S.Jr., and Steitz, T. A. (1978) Glucose-induced conformational change in yeast hexokinase. *Proc. Natl. Acad. Sci. U.S.A. 75*, 4848–4852.

(13) Gianni, S., Walma, T., Arcovito, A., Calosci, N., Bellelli, A., Engstrom, A., Travaglini-Allocatelli, C., Brunori, M., Jemth, P., and Vuister, G. W. (2006) Demonstration of long-range interactions in a PDZ domain by NMR, kinetics, and protein engineering. *Structure 14*, 1801–1809.

(14) James, L. C., Roversi, P., and Tawfik, D. S. (2003) Antibody multispecificity mediated by conformational diversity. *Science 299*, 1362–1367.

(15) Pan, H., Lee, J. C., and Hilser, V. J. (2000) Binding sites in *Escherichia coli* dihydrofolate reductase communicate by modulating the conformational ensemble. *Proc. Natl. Acad. Sci. U.S.A. 97*, 12020–12025.

(16) Cooper, A., and Dryden, D. T. (1984) Allostery without conformational change. A plausible model. *Eur. Biophys. J. 11*, 103–109.

(17) Lee, A. L., Kinnear, S. A., and Wand, A. J. (2000) Redistribution and loss of side chain entropy upon formation of a calmodulin-peptide complex. *Nat. Struct. Biol. 7*, 72–77.

(18) Gunasekaran, K., Ma, B., and Nussinov, R. (2004) Is allostery an intrinsic property of all dynamic proteins?. *Proteins 57*, 433–443.

(19) Henzler-Wildman, K. A., Lei, M., Thai, V., Kerns, S. J., Karplus, M., and Kern, D. (2007) A hierarchy of timescales in protein dynamics is linked to enzyme catalysis. *Nature 450*, 913–916.

(20) Jemth, P., and Gianni, S. (2007) PDZ domains: Folding and binding. *Biochemistry 46*, 8701–8708.

(21) Stiffler, M. A., Chen, J. R., Grantcharova, V. P., Lei, Y., Fuchs, D., Allen, J. E., Zaslavskaia, L. A., and MacBeath, G. (2007) PDZ Domain Binding Selectivity Is Optimized Across the Mouse Proteome. *Science 317*, 364–369.

(22) Saro, D., Li, T., Rupasinghe, C., Paredes, A., Caspers, N., and Spaller, M. R. (2007) A thermodynamic ligand binding study of the third PDZ domain (PDZ3) from the mammalian neuronal protein PSD-95. *Biochemistry 46*, 6340–6352.

(23) Fuentes, E. J., Gilmore, S. A., Mauldin, R. V., and Lee, A. L. (2006) Evaluation of energetic and dynamic coupling networks in a PDZ domain protein. *J. Mol. Biol. 364*, 337–351.

(24) Gianni, S., Engstrom, A., Larsson, M., Calosci, N., Malatesta, F., Eklund, L., Ngang, C. C., Travaglini-Allocatelli, C., and Jemth, P. (2005) The kinetics of PDZ domain-ligand interactions and implications for the binding mechanism. *J. Biol. Chem. 280*, 34805–34812.

(25) Bach, A., Chi, C. N., Olsen, B. T., Pedersen, W. S., Roder, U. M., Pang, F. G., Clausen, P. R., Jemth, P., and Strømgaard, K. (2008) Modified Peptides as Potent Inhibitors of the PSD-95/NMDA Receptor Interaction. *J. Med. Chem. 51*, 6450–6459.

(26) Chi, C. N., Engström, Å., Gianni, S., Larsson, M., and Jemth, P. (2006) Two conserved residues govern the salt and pH dependencies of the binding reaction of a PDZ domain. *J. Biol. Chem. 281*, 36811–36818.

(27) Fersht, A. (1999) Structure and Mechanism in Protein Science: A Guide to Enzyme Catalysis and Protein Folding , W. H. Freeman and Co., New York.

(28) Chi, C. N., Elfström, L., Shi, Y., Snäll, T., Engström, Å., and Jemth, P. (2008) Reassessing a sparse energetic network within a single protein domain. *Proc. Natl. Acad. Sci. U.S.A. 105*, 4679–4684.

(29) Malatesta, F. (2005) The study of bimolecular reactions under non-pseudo-first order conditions. *Biophys. Chem. 116*, 251–256.

(30) Zhang, Y., Dasgupta, J., Ma, R. Z., Banks, L., Thomas, M., and Chen, X. S. (2007) Structures of a human papillomavirus (HPV) E6 polypeptide bound to MAGUK proteins: Mechanisms of targeting tumor suppressors by a high-risk HPV oncoprotein. *J. Virol. 81*, 3618–3626.

(31) Liu, Y., Henry, G. D., Hegde, R. S., and Baleja, J. D. (2007) Solution structure of the hDlg/SAP97 PDZ2 domain and its mechanism of interaction with HPV-18 papillomavirus E6 protein. *Biochemistry 46*, 10864–10874.

(32) von Ossowski, I., Oksanen, E., von Ossowski, L., Cai, C., Sundberg, M., Goldman, A., and Keinänen, K. (2006) Crystal structure of the second PDZ domain of SAP97 in complex with a GluR-A C-terminal peptide. *FEBS J. 273*, 5219–5229.

(33) Grembecka, J., Cierpicki, T., Devedjiev, Y., Derewenda, U., Kang, B. S., Bushweller, J. H., and Derewenda, Z. S. (2006) The binding of the PDZ tandem of syntenin to target proteins. *Biochemistry 45*, 3674–3683.

(34) Kang, B. S., Cooper, D. R., Devedjiev, Y., Derewenda, U., and Derewenda, Z. S. (2003) Molecular Roots of Degenerate Specificity in Syntenin's PDZ2 Domain: Reassessment of the PDZ Recognition Paradigm. *Structure 11*, 845–853.

(35) Tungteakkhun, S. S., and Duerksen-Hughes, P. J. (2008) Cellular binding partners of the human papillomavirus E6 protein. *Arch. Virol. 153*, 397–408.

(36) Olson, S. T., Srinivasan, K. R., Bjork, I., and Shore, J. D. (1981) Binding of high affinity heparin to antithrombin III. Stopped flow kinetic studies of the binding interaction. *J. Biol. Chem. 256*, 11073–11079.

(37) Cui, Q., and Karplus, M. (2008) Allostery and cooperativity revisited. *Protein Sci. 17*, 1295–1307.

(38) Akke, M., Skelton, N. J., Kordel, J., Palmer, A. G.III, and Chazin, W. J. (1993) Effects of ion binding on the backbone dynamics of calbindin D9k determined by ^{15}N NMR relaxation. *Biochemistry 32*, 9832–9844.

(39) Malmendal, A., Evenas, J., Forsen, S., and Akke, M. (1999) Structural dynamics in the C-terminal domain of calmodulin at low calcium levels. *J. Mol. Biol. 293*, 883–899.

(40) Bracken, C., Carr, P. A., Cavanagh, J., and Palmer, A. G.III (1999) Temperature dependence of intramolecular dynamics of the basic leucine zipper of GCN4: Implications for the entropy of association with DNA. *J. Mol. Biol. 285*, 2133–2146.
(41) Mittermaier, A., and Kay, L. E. (2006) New tools provide new insights in NMR studies of protein dynamics. *Science 312*, 224–228.
(42) Freund, S. M., Johnson, C. M., Jaulent, A., and Ferguson, N. (2008) Moving towards High-Resolution Descriptions of the Molecular Interactions and Structural Rearrangements of the Human Hepatitis B Core Protein. *J. Mol. Biol. 384*, 1301–1313.
(43) Clarkson, M. W., and Lee, A. L. (2004) Long-range dynamic effects of point mutations propagate through side chains in the serine protease inhibitor eglin c. *Biochemistry 43*, 12448–12458.
(44) Tsai, C. J., del Sol, A., and Nussinov, R. (2008) Allostery: Absence of a change in shape does not imply that allostery is not at play. *J. Mol. Biol. 378*, 1–11.
(45) Doyle, D. A., Lee, A., Lewis, J., Kim, E., Sheng, M., and MacKinnon, R. (1996) Crystal structures of a complexed and peptide-free membrane protein-binding domain: Molecular basis of peptide recognition by PDZ. *Cell 85*, 1067–1076.
(46) DeLano, W. L. (2002) The PyMOL Molecular Graphics System , DeLano Scientific, San Carlos, CA.